

# Graphene Induced Diamond Nucleation on Tungsten

YONHUA TZENG <sup>1</sup> (Fellow, IEEE), AND CHIH-CHUN CHANG<sup>2</sup>

<sup>1</sup> Institute of Microelectronics, Department of Electrical Engineering, National Cheng Kung University, Tainan 70101, Taiwan

<sup>2</sup> Department of Electrical Engineering, National Cheng Kung University, Tainan 70101, Taiwan

CORRESPONDING AUTHOR: YONHUA TZENG (e-mail: tzengyo@gmail.com).

This work was supported by the Taiwan Ministry of Science and Technology under Grant MOST-106-2221-E-006-173-MY3.

**ABSTRACT** Chemical vapor deposition (CVD) of a diamond film on a non-diamond substrate begins with the insertion of diamond seeds or the formation of diamond nuclei on the substrate. For the deposition of a smooth, large-area and pin-hole free diamond film that adheres well to the substrate, diamond seeds or nuclei need to be of high density, uniformly distributed and adhere well to the substrate. Diamond seeding is not a diamond nucleation process. Bias enhanced nucleation (BEN) is the most effective means of heterogeneous nucleation of diamond for CVD diamond. It is based on a negative biasing voltage between the substrate and the diamond CVD plasma to accelerate positive ions from the plasma to bombard the substrate. Both direct diamond seeding and BEN have technical barriers in practical applications. New diamond nucleation techniques are desired. This paper reports novel heterogeneous diamond nucleation along edge line of graphene on tungsten leading to the deposition of continuous diamond films. Based on experimental observation, a diamond nucleation mechanism assisted by sp<sup>3</sup> C-W bonds at graphene edge is proposed. It is wished that scientists will become interested in revealing the precise diamond nucleation mechanism. With that, further optimization of this invention may lead to a new, complementary diamond nucleation process for practical deposition of diamond films.

**INDEX TERMS** Graphene, diamond, heterogeneous, nucleation, PECVD.

## I. INTRODUCTION

Diamonds exhibit many desirable properties, making them very promising materials [1]–[10]. Thermodynamically sp<sup>3</sup> bonded diamond is metastable while graphite is stable at atmospheric pressure and below. This makes the growth of diamond in laboratory chemical vapor deposition (CVD) reactors challenging [11]–[20]. On the contrary, 3-D graphite and 2-D graphene are sp<sup>2</sup> bonded carbon materials [21]–[23], which are thermodynamically stable at atmospheric pressure and below, making them easier than diamond to grow by laboratory CVD reactors. In order to deposit uniform, smooth, pin-hole free and large-area diamond films on non-diamond substrates by CVD techniques, it is necessary to either insert firmly diamond nanoparticles into the substrates or form diamond nuclei on the substrates. Uniform and high-density diamond seeds or diamond nuclei are prerequisite. Diamond seeding is effective for depositing CVD diamond films for many applications. However, diamond seeds need to be pre-synthesized.

Detonation nanodiamond particles are often used as diamond seeds. Therefore, diamond seeding is not a diamond nucleation process. For complex and irregular shaped substrates, uniform seeding of nanodiamond is challenging. Alternative means of creating diamond seeds on the substrates are needed. Formation of high-density diamond nuclei which adhere well to non-diamond substrates, where diamond films are to be deposited is thus important to practical application of CVD diamond films.

Enhancement of diamond nucleation using carbon-based materials have been widely reported because mainly diamond is a crystalline carbon. On diamond seeded silicon substrates, the coating of amorphous carbon was reported to result in an increased diamond nucleation density under Plasma CVD conditions [24]. Amorphous carbon protects pre-planted diamond seeds from being etched away or losing adhesion to the substrates by the hydrogen-rich plasma. Etching of amorphous carbon by atomic hydrogen also produces carbon

containing radicals, such as methyl radicals, which may re-insert into  $sp^3$  bonded diamond seeds or create new diamond nuclei.

Without diamond seeding, carbon-based materials also enable diamond nucleation without pre-seeding of diamond. For example, nucleation of diamond without diamond seeding at edges and surface steps of graphite and graphite-like structures, and conversion of amorphous carbon clusters with mixed  $sp^2$  and  $sp^3$  bonded carbon phases into diamond nuclei have been reported. A variety of mechanisms cause three-dimensional and low-dimensional carbon to enhance diamond nucleation. For example, diamond nucleates on graphite by heteroepitaxial insertion of carbon containing radicals to steps and edges of graphite [25]–[28]. Heteroepitaxial nucleation of diamond on some non-carbon crystals has also been reported [29]–[31]. The size of heteroepitaxial diamond is controlled by the availability of large-area substrates which are suitable for heteroepitaxial growth of diamond. Graphite is a three-dimensional precursor for diamond nucleation. Although multi-layer graphene and multi-wall CNT are sometimes considered 2-D and 1-D materials, the involvement of many graphitic layers in the heteroepitaxial nucleation and growth makes them really three-dimensional nucleation processes. Monolayer graphene and single-wall CNT enabled diamond nucleation would be true 2-D and 1-D diamond nucleation processes.

After multiwall CNT (MWCNT) and amorphous carbon are melted by laser or electron beam to form a super undercooling state, mixed-phase carbon and nanodiamond particles form in the solidification process [32], [33]. Many nanodiamond particles were observed along MWCNT. The equivalent nucleation density calculated by the distance between one-dimensional array of nanodiamond particles which form along MWCNT was reported to be on the order of  $10^{10} \text{ cm}^{-2}$ . Diamond nuclei must adhere well to the substrate where a diamond film will be deposited. If uniform and high-density MWCNT can cover and adhere well to the substrate for diamond film deposition, this diamond nucleation process will be useful. However, laser melting of large-area MWCNT covered substrates takes time. With free-standing MWCNT, further growth of diamonds from diamond nuclei formed on MWCNT might cause MWCNT to be etched and diamonds nuclei and diamond they form lose adhesion to the MWCNT and the substrate.

Amorphous carbon clusters with mixed  $sp^2$  and  $sp^3$  bonded carbon exhibit effective enhancement in diamond nucleation. A part of carbon atoms in these clusters are  $sp^3$  bonded, which matches diamond structure. This is especially true when atomic hydrogen plays active roles in etching non-diamond carbon, terminating carbon dangling bonds, and abstraction of atomic hydrogen. Under the typical diamond CVD conditions in the presence of atomic hydrogen, the etch rate of non-diamond carbon is faster than that of diamond. Non-diamond carbon is etched by atomic hydrogen to form carbon-containing radicals such as  $\text{CH}_3$  [34] and  $\text{C}_2$  [35], [36], which are known to be two major radicals for diamond nucleation and growth.  $\text{C}_2$  also induce secondary nucleation on

existing diamond grains. Ultrananocrystalline diamond (UNCD) grains of 2–5 nm in size are formed by secondary nucleation and are surrounded by mixed-phase amorphous carbon. Under proper conditions, some carbon-containing radicals might insert in the mixed phase carbon cluster again. If the insertion of carbon-containing radicals forms additional  $sp^3$  carbon-carbon bonds to an existing carbon clusters with diamond-like structures, the size of the diamond embryo increases and becomes more stable. When the process continues, stable diamond nuclei might be formed from the originally mixed phase carbon clusters.

Most of the transformation of mixed-phase amorphous carbon clusters to diamond nuclei is aided by atomic hydrogen produced by plasma assisted and hot-filament CVD processes. In some cases, such as flame assisted diamond growth, OH radicals play roles of atomic hydrogen. Atomic hydrogen, for example, preferentially etches non-diamond-bonded carbon to form carbon-containing radicals, stabilizes diamond-phase carbon, abstracts surface atomic hydrogen, and creates active carbon sites for insertion of carbon-containing radicals. Therefore, diamond nucleation mechanism for these examples is not direct solid-state conversion of amorphous carbon into diamond. Three-dimensional amorphous carbon clusters act as the precursors for enhancing the diamond nucleation.

Amorphous carbon clusters favorable for diamond nucleation are formed by many different ways including, for example, ion irradiation of carbon fibers, CNT [37], and amorphous carbon [38], UV laser annealing of carbon films [39] and bias-enhanced nucleation (BEN) at the aid of atomic hydrogen and under diamond CVD conditions [20], [38], [40]–[42].

Diamond nucleation depends on both different forms of carbon precursors and different forms of energy inputs. Large-volume plasma, arc jet, ion beam, combustion flame, and laser assisted CVD processes are among reported energy sources for the creation of radicals responsible for diamond nucleation. Very high-power-density energy inputs, such as pulsed laser may cause carbon precursors to melt. After carbon reaches super undercooling conditions by the laser beam illumination, the solidification process may lead to the conversion of amorphous carbon [32] and multi-layer CNT [37] into diamond nuclei. However, diamond nucleation by this kind of processes faces challenges in the deposition of adhesive diamond films on large-area non-diamond substrates.

High-to-medium power-density energy inputs such as arc jets create high temperature thermal plasma, which generates high concentration atomic hydrogen and carbon containing radicals. This is favorable for achieving super-saturation of carbon vapor for subsequent diamond nucleation or the formation of graphite and multilayer graphene for heteroepitaxial nucleation of diamond at edges and surface steps. The extent of supersaturation of carbon vapor depends on the solid solubility of carbon in the substrate. The less the carbon solid solubility a substrate has, the higher the probability for graphite-like multi-layer or many-layer graphene to form on the substrate. Carbon solubility in copper is much lower than that in metal iron. As a result, the density of diamond

nucleation on copper is higher than that on metal. High concentration carbon dissolves in nickel at a high temperature and diffuses outwards to the surface when it cools down. The outward diffusion of carbon forms multilayer graphene, which enhances diamond nucleation under hydrogen-rich diamond CVD conditions [43].

Combustion flame CVD [44]–[46] of diamond on copper and sintered WC with 6% Co has been demonstrated without applied negative biasing voltage and direct seeding of nanodiamond. Arc jets and combustion flame used for diamond nucleation and growth are more difficult to scale up for large-area substrates compared to volume discharge plasma. Diamond nucleation on WC with 6% cobalt suffer from poor adhesion to the substrate.

Amorphous carbon may contain different percentage of sp<sup>3</sup> carbon-carbon bonds. It ranges, for example, from nearly all sp<sup>3</sup>-bonded tetrahedral-amorphous carbon (TaC) [47] to randomly packed carbon clusters. Diamond-like-carbon (DLC) is commonly used to describe amorphous carbon exhibiting many similar properties of diamond and containing mixed sp<sup>2</sup> and sp<sup>3</sup> carbon-carbon bonds. Some DLC films contain atomic hydrogen, which terminates carbon dangling bonds and assists in stabilizing sp<sup>3</sup> bonds. Since diamond nucleates from carbon, DLC containing sp<sup>3</sup> carbon-carbon bonds is a natural candidate for enhancing diamond nucleation. There are many reports about the enhancement of diamond nucleation by mixed-phase amorphous carbon clusters.

For applications to large-area diamond coatings with strong adhesion, diamond nuclei must adhere well to the non-diamond substrate on which a diamond film is to be coated. If nucleation of diamond is based on amorphous carbon clusters without strong adhesion to the substrate, the deposited diamond films do not adhere well to the substrate. Bias enhanced nucleation of diamond first reported by Yugo et al. [40] resorts to in-situ ion bombardment of amorphous carbon, which is simultaneously deposited by the diamond CVD plasma on the substrate. Ion bombardment creates transient high-temperature and high-pressure conditions for mixed-phase sp<sup>2</sup> and sp<sup>3</sup> bonded carbon clusters to be deposited. In the aid of atomic hydrogen and energy input from the plasma and ion bombardment, sp<sup>2</sup> bonded carbons are etched at a higher rate compared to sp<sup>3</sup> bonded carbons. The content of sp<sup>3</sup> bonded carbon structures survive and evolve into diamond nuclei. DC plasma nucleation and growth of diamond on substrates placed on the anode has ion bombardment of the substrate like the BEN process. It was reported by Kazuhiro Suzuki et al. [48] to induce diamond nucleation. Energy of ions bombarding the anode is lower than that on the cathode. Diamond bonds are damaged by ions bombarding the cathode but not the anode. In both cases, the negative potential difference between the substrate (or at the anode of DC plasma) and the plasma supplies energy to the ions bombarding the substrate. In contrast to BEN, high flux of low energy ion bombardment might promote the formation of multilayer graphene and graphite. The optimal ion energy is higher than what is required to create sp<sup>3</sup> carbon bonds in the carbon clusters but lower than what would break sp<sup>3</sup> diamond bonds.

Abundant CH<sub>3</sub> and C<sub>2</sub> radicals are produced by high-temperature plasma generated by high power density at a high gas pressure. High concentration of carbon containing radicals facilitate diamond nucleation on mixed-phase carbon clusters, multi-layers graphene, and graphite flakes. These are precursors for diamond nucleation. For both BEN and DC PECVD, electric fields induced by a negative voltage to the substrate with respect to the plasma accelerate positively charged ions, including hydrogen ions and ionized carbon radicals, to bombard the carbon clusters on the substrate. The ion energy depends on the negative bias voltage and the extent of energy loss by ions in their trip on the way from the plasma to the substrate. Collisions of ions causes ion energy to be shared with particles they collide. When the bias voltage is properly adjusted, ions does not damage diamond bonds of an early-stage diamond nucleus obtain adequate energy to break sp<sup>2</sup> carbon-carbon bonds for sp<sup>2</sup> bonded carbon to be etched away or converted into sp<sup>3</sup> diamond bonds. At the same time, atomic hydrogen etches diamond at a much lower rate than non-diamond carbon phases. The etched non-diamond carbon becomes carbon-containing radicals, which later insert into the carbon cluster with a finite probability of forming sp<sup>3</sup> diamond bonds. The energy input from ion bombardment and the reactions of the carbon clusters with the substrate at the elevated CVD temperature result in chemical bonding between the diamond nuclei and the substrate. Diamond coatings originating from these diamond nuclei adhere well to the substrate for a strong diamond coating.

Most of lab CVD conditions at near- or sub-atmospheric gas pressure and near- or below 1000 °C temperature are in favor of graphite growth over diamond because graphite is thermodynamically stable while diamond is metastable. However, etching of non-diamond-bonded carbon from an existing carbon cluster with mixed sp<sup>2</sup> and sp<sup>3</sup> bonded carbon and subsequent insertion of carbon containing radicals in the form of sp<sup>3</sup> bonding to active carbon sites on the carbon clusters leads to finite probability of building sp<sup>3</sup> bonded diamond structures as part of the carbon cluster. When this process is assisted by chemical, for example, atomic hydrogen and OH radicals, stabilization of carbon dangling bonds, the possibility of converting the sp<sup>3</sup> carbon-H bonds to sp<sup>2</sup> carbon-carbon bonds is suppressed even under the pressure-temperature conditions where graphite is more energetically favorable than diamond. The subsequent abstraction or thermal desorption of the terminating atomic hydrogen creates opportunity for carbon-containing radicals, such as CH<sub>3</sub> and C<sub>2</sub>, to be inserted to the diamond-bonded sp<sup>3</sup> structure, which is stabilized by hydrogen termination to surface carbon atoms and by the remaining carbon cluster with mixed sp<sup>2</sup> and sp<sup>3</sup> carbon-carbon bonds.

The primary originality of this paper is the introduction of monolayer graphene on W surface to enhance nucleation along graphene edges created by hydrogen-rich plasma etching of the monolayer graphene. Because diamond is made of carbon, it is natural that most reported non-epitaxial diamond nucleation is carbon-based. Furthermore, diamond is a sp<sup>3</sup> bonded carbon crystal, and, therefore, except

heteroepitaxial diamond nucleation on non-carbon crystals, all diamond nucleation uses carbon-based materials. Although monolayer graphene is also a carbon material, it is only one atom thick and very different from graphite in many aspects of physical and chemical properties. Besides three-dimensional amorphous carbon and graphite enhanced diamond nucleation, direct conversion to diamond and enhancement in diamond nucleation by low dimensional carbon have attracted increasing attention in recent years. Among low-dimensional carbon, fullerene [49], CNT and carbon fiber [50], and graphene [51] are among most interesting candidates to diamond CVD scientists and technologists.

The state-of-the-art diamond CVD technology mainly applies the following diamond seeding and BEN for providing the initial diamond, i.e., diamond seeds or nuclei on non-diamond substrates. The diamond seeds and nuclei grow larger in size to form a diamond coating for applications. The first method directly inserts nano-scale diamond particles into the substrate. Diamond nanoparticles are either crushed from larger diamond crystals or synthesized directly in detonation environments. The challenge is how to insert dense diamond seeds firmly, and uniformly on complex surfaces of non-diamond substrates.

The second commonly adopted method relies on energetic ion bombardment of the carbon clusters being deposited on a non-diamond substrate. A negative voltage is applied to the substrate with respect to the plasma. Positive ions are accelerated by the electric field in an orientation perpendicular to the substrate surface. Scattering by gas molecules results in the spreading of ion energy being transferred to carbon clusters. By controlling the negative bias voltage and the flux of positive ions, sp<sup>3</sup> bonded carbon clusters are formed among other carbon phases on the substrate. Typically, a negative bias voltage of 100–200 V is applied to an electrically conductive substrate surface. For electrically insulating substrates, applying radio frequency (RF) power to the substrate with respect to the plasma results in RF induced negative DC bias in the time averaged scale to the substrate due to different speeds of electrons and ions in the plasma. Plasma chemistry plays the next important role of suppressing the formation or the etching of non-diamond carbon phases while preferentially allowing diamond nuclei to be formed and grow.

Since the electric field created by the applied negative bias voltage to the substrate aims between the plasma and the substrate, it is perpendicular to the substrate. Ion bombardment of non-planar and complex substrates is therefore non-uniform. For example, the ion flux arriving at the side walls of a deep trench in a planar substrate is much lower than that at the bottom. Diamond nucleation on these side walls by bias enhanced nucleation method is therefore relatively ineffective.

For diamond nucleation and growth under thermodynamically metastable conditions in a laboratory reactor, the dangling bonds on the growth front of a diamond surface tend to form sp<sup>2</sup> carbon-carbon double bonds. Once a sp<sup>2</sup> bond is formed, converting it to a sp<sup>3</sup> bond takes additional energy. A proper amount of atomic hydrogen plays a passivation role effectively. Atomic hydrogen atoms from the plasma terminate

and satisfy the dangling bonds of diamond surface carbon. However, once a dangling bond is terminated by a hydrogen atom, carbon containing radicals cannot insert to the diamond surface for the diamond to grow. If the atomic hydrogen flux is too high, carbon atoms on diamond surface may be etched. Therefore, a delicate balance between adsorption and desorption and the abstraction of atomic hydrogen on diamond surface is required.

Thermal desorption and abstraction of atomic hydrogen which passivates diamond surface by the incoming atomic hydrogen from the plasma to form molecular hydrogen help create active carbon sites for carbon radicals to insert to the diamond. If there are too many active carbon sites, neighboring carbon dangling bonds may form sp<sup>2</sup> carbon-carbon bonds before a carbon radical becomes available to replace the atomic hydrogen termination. If there are few active carbon sites for carbon radicals to adsorb, the diamond growth rate is low. In brief, special chemical environments are required to provide proper amount of atomic hydrogen for desired diamond growth while preventing reactive carbon dangling bonds on diamond surface from forming thermodynamically more favorable graphitic sp<sup>2</sup> carbon-carbon double bonds.

Uniformly distributed diamond nuclei of a high number density are desirable for growing diamond structures with smooth surfaces on large-area substrates [11]–[20]. Besides, discrete nano-scale diamond crystals are excellent drug delivery vehicles because of their long-term biochemical compatibility and convenient functionalization of their surfaces for carrying drug molecules [8]. Diamond is chemically inert and does not react with any chemical at room temperature. Ultra-nano-crystalline-diamond coated dental implants and artificial retinal provide promising long-term safety for the health care industry [52]. A wide variety of practical applications of CVD diamond made in laboratory reactors have been produced to take advantage of its excellent physical, chemical, thermal, optical, electronic, mechanical, and tribological properties [1]–[5].

When coarsely distributed diamond seeds suffice, mechanical scratching of a substrate and the coating with carbide forming metals have been reported to promote heterogeneous diamond nucleation. Micron-sized diamond powder can also be used to polish a substrate. The polishing action causes diamond edges to break off. Diamond debris inserts in the substrate and serves as a diamond seed. However, these methods produce diamond nuclei which are too low in the number density than the two most commonly applied diamond nucleation methods in modern diamond technology, i.e., bias enhanced nucleation (BEN) [19], [20] and nanodiamond seeding [52].

Nanodiamond seeding involves the placing and adhesion of a monolayer of high number-density diamond nanoparticles on a non-diamond substrate. An adhesion promoting buffer layer such as amorphous carbon helps the retention of diamond seeds during initial stage of PECVD diamond growth when diamond seeds may lose adhesion to the substrate or be etched away by the hydrogen-rich plasma. When closely spaced nanodiamond particles inserted in a substrate grow bigger, they merge to form a continuous diamond film. The

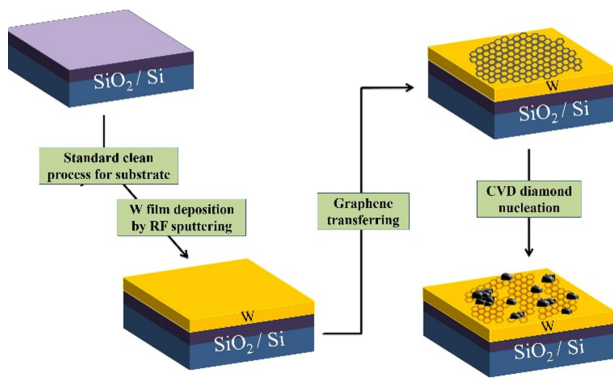


**FIGURE 1.** Schematic diagram of a chemical diamond nucleation process.

technical challenge is how well one can uniformly insert high-density nanodiamond seeds on complex non-planar, and large-area substrates.

BEN has technical barriers, too. The ion flux and ion energy in a plasma CVD reactor depend on geometrical parameters besides the applied negative biasing voltage. For example, the sidewalls of a narrow trench are not subjected to ion bombardment because the sidewalls are parallel to the direction of ion velocity. The biasing electric field is perpendicular to the bottom surface. Ions are accelerated in the direction of the electric field. Therefore, the bottom of a trench is bombarded by incident positive ions.

Recent advancement in graphene manufacturing technology has led to direct conversion of bi-layer graphene to single-layer fluorinated diamond. Few-layer graphene has also been reported to form ultra-thin  $sp^3$  bonded diamond phases [53], [54]. However, these exciting progresses in ultra-thin diamond phases, which are achieved from bi-layer and few-layer graphene are of little use for the deposition of large-area CVD diamond films. Diamond formed by these means are easily etched away by hydrogen-rich plasma. Therefore, the invention of novel chemically induced generation of diamond nuclei, which are stable in diamond PECVD environments for further growth to form continuous diamond films is highly desirable. Such novel chemical nucleation of diamond might overcome some technological barriers of traditional BEN and nanodiamond seeding methods of diamond nucleation.

In this paper, we report the invention of monolayer graphene induced diamond nucleation on tungsten metal.  $SiO_2$  surface is coated with a tungsten thin film followed by the coverage by one or more transferred layers of monolayer graphene. Neither diamond seeding nor bias enhanced nucleation is applied.

## II. METHODS AND PROCEDURES

Figure 1 shows a schematic flow chart of the synthesis of diamond nuclei on graphene covered tungsten on  $SiO_2$  surface. Monolayer graphene is synthesized by a traditional thermal CVD process in methane diluted by hydrogen and argon [6]. Tungsten (W) thin film is deposited by means of RF magnetron sputtering technique. Graphene grown on a copper foil

is transferred to a tungsten coated  $SiO_2$  substrate. Microwave plasma CVD technique is applied for diamond nucleation and growth. Further growth of diamond grains leads to the formation of a continuous diamond film.

A computer-controlled Lambda microwave plasma CVD system is used for diamond nucleation and growth. The diamond CVD plasma is excited by 915 MHz microwave. The system has an 8"-diameter substrate holder. Plasma is generated in gas mixtures of 1–3% methane diluted by 99–97% hydrogen. Microwave power of 3000–6000 W at 915 MHz is applied at 50 Torr gas pressure. The substrate temperature is measured by a dual-color optical pyrometer. The substrate temperature readout is 950 °C when the plasma is turned on, and 850 °C immediately after the plasma is turned off.

Tungsten is sputter deposited on substrates by an RF magnetron sputtering system operating at a gas pressure below 30 mTorr in argon gas. The substrate holder rotates for more uniform deposition. The RF power is 30 W–200 W at 13.56 MHz. A quartz crystal balance is used to monitor the thickness of the deposited tungsten thin film.

Synthesis process for graphene has been reported in [6]. In brief, graphene is synthesized by a low-pressure thermal CVD technique. Methane diluted by hydrogen and argon is applied to synthesize graphene on copper foils at 1040 °C. Monolayer graphene is evaluated by means of a back-gate FET. Field-effect carrier mobility is measured to be 414  $cm^2/Vs$ . The monolayer graphene used for diamond nucleation is of good quality [6].

## III. RESULTS AND DISCUSSION

Figure 2(A) shows a Raman spectrum measured from a  $SiO_2$  substrate, to which a thermal CVD monolayer graphene has been transferred. RF magnetron sputtering technique is applied to deposit tungsten on  $SiO_2$ . Graphene is synthesized on a copper foil by a thermal CVD technique using methane gas diluted by hydrogen and argon at the substrate temperature of 1040 °C. The monolayer graphene exhibits a G-band at  $1586\text{ cm}^{-1}$  and a 2D-band at  $2680\text{ cm}^{-1}$  with little D-band signal in the Raman spectrum excited by a 532-nm laser. The Raman spectrum and the well-studied self-limiting surface diffusion model for graphene synthesis on copper by thermal CVD indicate that the graphene is monolayer and of high quality [55]. After the copper foil is etched away, graphene is transferred from the copper foil to the destination substrate. Both polymer-assisted graphene transfer methods and a polymer-less graphene transfer method are applied [56], [57]. Although the graphene transfer process does leave some residues on the graphene and between the graphene and the destination substrate, the transfer process is tedious but does not affect adversely on the diamond nucleation. The residues are rapidly etched by the hydrogen-rich plasma and vaporized at the high temperature of diamond PECVD process.

Figure 2(B) shows an optical emission spectrum (OES) of the diamond PECVD plasma. The graphene covered and W coated  $SiO_2$  substrate is exposed to microwave plasma in 1%  $CH_4$  diluted by hydrogen for in-situ diamond nucleation and growth. The OES shows that the diamond CVD plasma

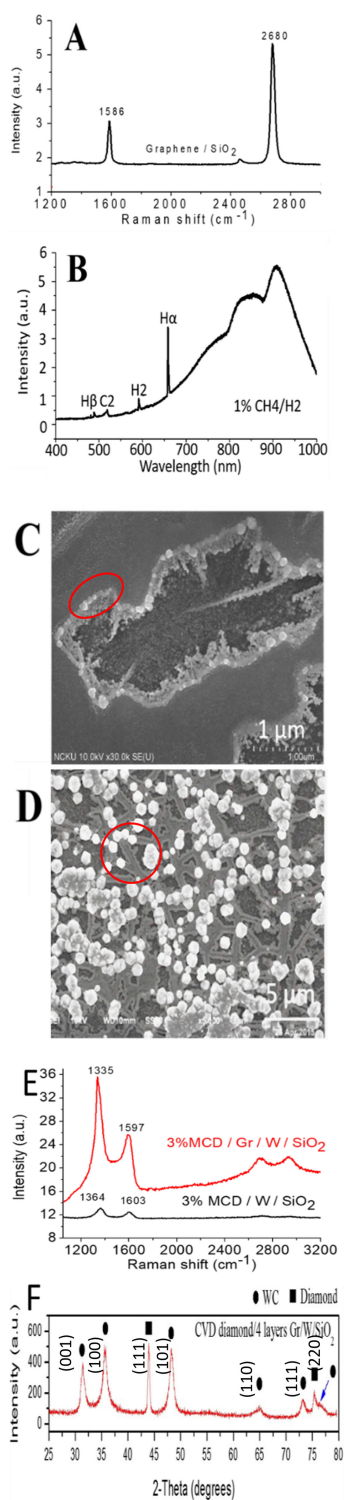


**FIGURE 2.** (A) Raman spectra of monolayer graphene on  $\text{SiO}_2$ . (B) Optical emission spectrum of diamond CVD microwave plasma in 1%  $\text{CH}_4$  diluted by  $\text{H}_2$ . (C) Diamond nuclei form along the edge of an etched hole of the monolayer graphene. Diamond nanoparticles grown from diamond nuclei are highlighted by a red circle. (D) Holes are etched in the monolayer graphene to form a 2-D network of graphene ribbons exhibiting many holes and clusters of diamond crystals form along edges of the graphene holes. Graphene ribbons are highlighted by a red circle. (E) Raman spectra of diamond nucleation on W coated  $\text{SiO}_2$  with graphene coverage (upper, red) and without graphene coverage (lower, black). (F) X-ray diffraction spectrum of CVD diamond on graphene covered and W coated  $\text{SiO}_2$ .

has abundant atomic hydrogen represented by the strong  $\text{H}_\alpha$  peak. The strong background signal in the long-wavelength range is caused by blackbody radiation from the heated high-temperature substrate surface under diamond PECVD conditions. To confirm reproducibility of the diamond nucleation plasma conditions, OES is measured for every experiment as a comparison.

Figure 2(C) shows the SEM image of an atomic hydrogen etched hole in a monolayer graphene covering tungsten coated  $\text{SiO}_2$ . A red color circle highlights an array of diamond nuclei along the edge of the graphene hole. The distance between two neighboring diamond nuclei is about  $0.1 \mu\text{m}$ . This indicates a possible high nucleation density of  $10^{10} \text{cm}^{-2}$ . The image clearly displays many more diamond nuclei and some larger diamond grains along and near the graphene edges. The larger diamond grains are the grown-up version of the early-bird diamond nuclei. The graphene surface which is not etched appears smooth without diamond nucleation. The diamond CVD plasma in 1% methane diluted by 99% hydrogen begins to react with and etch the monolayer graphene most likely from defects and domain boundaries to form multiple etched holes. Remaining unetched graphene that surrounds etched holes forms a mesh-like network consisting of graphene micro-ribbons with abundant edges. Graphene micro-ribbons are highlighted by a red-color circle in Fig. 2(D). After diamond nuclei are formed at edges of graphene holes, the width of a graphene micro-ribbon decreases further due slow but continuous etching by atomic hydrogen. New graphene edges are exposed for more diamond nucleation. As a result, 2-D distribution of diamond nuclei on the substrate can be formed. High quality graphene survives the diamond CVD plasma and protects tungsten underlayer from forming tungsten carbide. The exposed tungsten inside etched graphene holes forms tungsten carbide by reacting with carbon radicals from the diamond PECVD plasma. The etched graphene holes are surrounded by graphene edges with highly reactive dangling bonds. Most of these dangling bonds are terminated by atomic hydrogen. Some of these dangling bonds have the terminating atomic hydrogen thermally desorbed or abstracted by incoming atomic hydrogen from the plasma. These carbon atoms at graphene edges with unsatisfied dangling bonds are active sites for reacting with tungsten atom to form C-W bonds or reacting with incoming carbon containing radicals from the plasma to form  $\text{sp}^3$  C-C bonds. The W-C bonds may force the graphene edges to rise from the substrate surface. The original 2-D graphene edges thus become parts of 3-D structures. Under favorable conditions, some C-C-W  $\text{sp}^3$  bonded 3D structures may induce chain reactions for many more additional carbon radicals such as methyl radicals to be inserted to the 3-D tungsten supported  $\text{sp}^3$  carbon structures leading to the formation of stable diamond nuclei. The precise mechanism leading to the observed diamond nucleation along edges of monolayer graphene covering tungsten under hydrogen-rich diamond CVD plasma environment is not clear yet. After extensive discussion with diamond and graphene theoreticians, it is considered that the proposed tungsten

assisted heterogeneous diamond nucleation mechanism is possible but needs further study for confirmation. We hope that the report of confirmed experimental result can inspire scientists to reveal the most possible routes to monolayer graphene induced diamond nucleation on tungsten metal.

Figure 2(D) shows an SEM image of diamond grains around graphene micro-ribbons. A network of 2-D graphene micro-ribbons are shown in the background of the image of diamond grains. The graphene-ribbon mesh includes many holes of etched graphene as shown in Fig. 2(C). Since diamond nucleation occurs at edges of etched graphene holes, the total length of graphene edges needs to be as large as possible. This can be achieved by randomly stacking multiple individual graphene-ribbon meshes one on top of the other on tungsten metal. The stacked monolayer graphene is different from multi-layer graphene because of the random stacking of monolayer graphene layers. As the total length of graphene edges, which are in contact with tungsten increases, so does the density of diamond nuclei.

Multilayer graphene covered tungsten does not enhance as much diamond nucleation as randomly stacked monolayer graphene. The edge structures of multi-layer graphene are more complicated than that of monolayer graphene. The reactions of edge carbons of monolayer graphene with tungsten are, therefore, different from those of multi-layer graphene. Multi-layer graphene and graphite have been reported to enhance diamond nucleation by means of heteroepitaxial nucleation and growth of diamond at graphite edges and steps on the basal plane of graphite flakes. Similar mechanism applies to many-layer graphene, which is practically ultra-thin graphene.

Figure 2(E) shows a Raman spectrum (upper spectrum in red color) measured from diamond nuclei formed on graphene covered and tungsten coated SiO<sub>2</sub> surface. In this case, the diamond nucleation is carried out by microwave plasma in 3% methane diluted by 97% hydrogen. The co-existence of diamond nuclei and small diamond grains results in a broadened diamond Raman peak around 1335 cm<sup>-1</sup>. The spectrum exhibits a strong and clear Raman G-band signal originating from graphene which is not etched by the diamond PECVD plasma. As a comparison, Fig. 2(E) also shows a Raman spectrum (lower spectrum in black color) measured on the surface of a tungsten coated SiO<sub>2</sub> substrate without coverage by monolayer graphene. After exposure to the same diamond PECVD plasma, the Raman spectrum measured from the tungsten coated substrate without graphene does not show any sign of the diamond Raman peak. Tungsten metal alone is not as effective as graphene covered tungsten in inducing diamond nucleation.

Figure 2(F) shows an X-ray diffraction pattern for a diamond film grown on tungsten coated SiO<sub>2</sub>. Four layers of individual monolayer graphene are stacked randomly on the tungsten film. The diffraction pattern includes both tungsten carbide and diamond diffraction peaks. Although this result is not sufficient to prove the proposed mechanism of diamond nucleation via reactions between graphene and tungsten to

form C-W bonds in the diamond CVD plasma, it does serve as an evidence of the formation of tungsten carbide, mostly in etched graphene holes.

The precise mechanism for monolayer graphene induced diamond nucleation on tungsten coated silicon substrate needs further study to understand. A reaction route is proposed, by which carbon atoms at graphene edges react with tungsten to form sp<sup>3</sup> C-W bonds. When chain reactions occur and additional carbon containing radicals, such as CH<sub>3</sub> methyl radical, supplied by the PECVD plasma in methane diluted by hydrogen insert to the C-W bonds, sp<sup>3</sup> bonded diamond structure might be forms. Further growth of the diamond structure forms stable diamond nuclei. Carbon atoms along graphene edges can be terminated by atomic hydrogen supplied by the hydrogen-rich diamond PECVD plasma. These hydrogen atoms can be abstracted by arriving flux of hydrogen atoms from the plasma to form hydrogen molecules leaving active carbon sites with dangling bonds for carbon containing radicals to insert. The dangling bonds can also be satisfied by tungsten atoms to form sp<sup>3</sup> C-W bonds. A C-W sp<sup>3</sup> bond lifts the carbon atom at graphene edge. The carbon atom at the graphene edge can accept methyl radical from the plasma. Hydrogen atoms of the added methyl radical can in turn be abstracted by atomic hydrogen to expose active sites for further formation of C-C sp<sup>3</sup> bonds. It is hoped that computational scientists familiar with molecular dynamic simulation and other suitable computational techniques can perform theoretical studies of the nucleation mechanism.

Figure 3 shows diamond nuclei induced by two, three, and four randomly stacked individual layers of monolayer graphene. Graphene is transferred one at a time and stacked on top of the other on tungsten coated SiO<sub>2</sub>. Individual layers of monolayer graphene are stacked in such a way that the upper layer graphene covers only part of the lower layers of graphene. The new graphene covered area has one more stacked layer of monolayer graphene. The area where the upper layer graphene does not cover have one less stacked layers of graphene. Fig. 3(A) shows that different areas on the tungsten coated SiO<sub>2</sub> substrate are covered by one, two, three and four individual layers of monolayer graphene. Some areas are left without graphene coverage. This substrate with different numbers of stacked monolayer graphene is used to confirm the relationship of diamond nucleation density with the number of stacked monolayer graphene. When individual layers of monolayer graphene are stacked, plasma etching produces multiple meshes of graphene micro-ribbons which overlap on each other to form a joint mesh with more holes and longer graphene edges. More graphene edges around these holes result in more diamond nuclei.

Figure 3(B) shows Raman spectra of randomly stacked monolayer graphene indicating that monolayer graphene is of high quality. The randomly stacked monolayer graphene exhibits a Raman spectrum, which is like that of a single monolayer graphene. Raman spectra of diamond films grown using 1, 2, 3, and 4 stacked layers of individual monolayer graphene show slightly shifted diamond peak at 1334 cm<sup>-1</sup>.

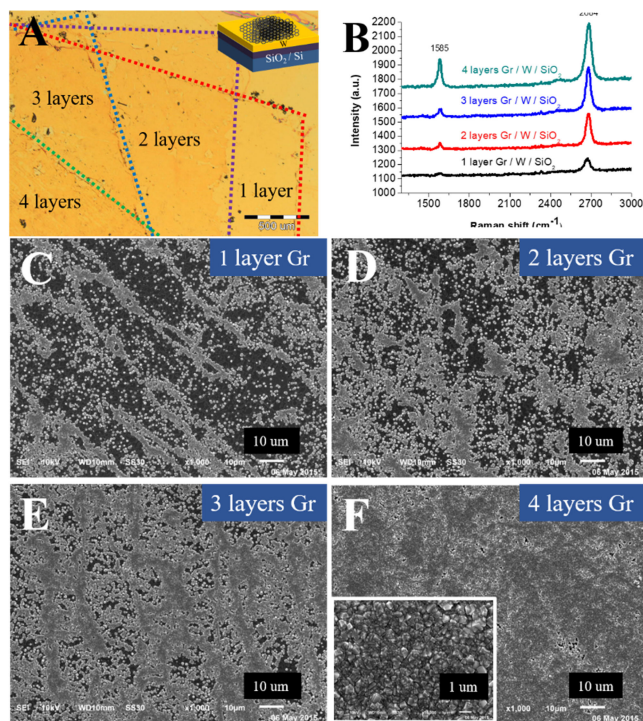


**FIGURE 3.** Diamond nucleation and growth in 1% CH<sub>4</sub> diluted by hydrogen on varied layers of graphene covered tungsten coated SiO<sub>2</sub>. (A) Intentionally misaligned stacking of four layers of monolayer graphene on W coated SiO<sub>2</sub>. The misalignment results in different areas of the SiO<sub>2</sub> being covered by one, two, three, and four or no graphene. (B) Raman spectra of one, two, three, and four layers of stacked monolayer graphene on W coated SiO<sub>2</sub>. (C) Low diamond nucleation density in the area with one layer of graphene coverage. (D) Medium diamond nucleation density in the area with two layers of graphene coverage. (E) High diamond nucleation density in the area with three layers of graphene coverage. (F) Almost pinhole free diamond nucleation density in the area with four layers of graphene coverage.

Graphene covered and tungsten coated SiO<sub>2</sub> is exposed to diamond CVD plasma in 1% CH<sub>4</sub> diluted by 99% hydrogen for 4 hr. Figs. 3(C, D, E, F) shows SEM images of diamond deposited by the aid of 1, 2, 3, and 4 randomly stacked layers of monolayer graphene. The density of diamond nucleation increases with the number of stacked monolayer graphene. Under the diamond CVD conditions, four layers of stacked monolayer graphene produce the highest density of diamond nuclei and grains among these samples. Figure 3(F) shows that there are no pinholes in the diamond film deposited from diamond nuclei formed by the aid of four randomly stacked layers of monolayer graphene on tungsten coated substrates. No diamond seeding and bias enhance diamond nucleation were applied.

Figure 4 shows continuous diamond films grown by PECVD in 3% methane diluted by hydrogen on graphene covered tungsten on SiO<sub>2</sub> substrates. Tungsten coated silicon substrates are covered by 2, 3, and 4 individual layers of monolayer graphene. The higher diamond nucleation achieved by 4 layers of graphene is shown by the smallest grain sizes in the polycrystalline diamond film. Raman spectra

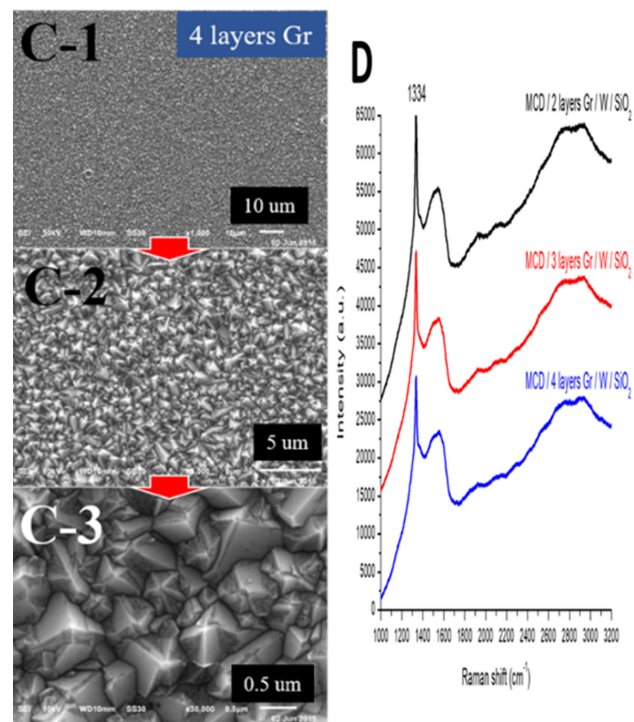
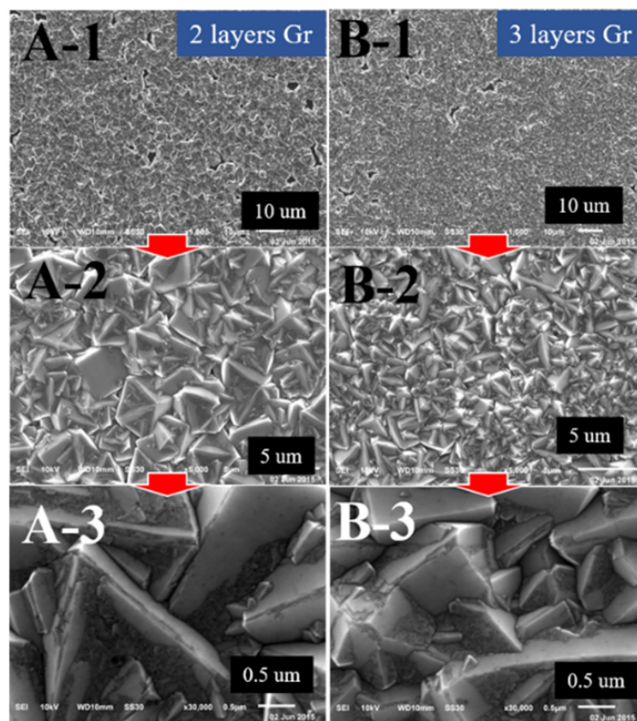


**FIGURE 4.** Diamond films nucleated and grown in 3% CH<sub>4</sub> diluted by hydrogen for 4 hr at 50 Torr gas pressure and 900 °C substrate temperature. (A) A diamond film nucleated and grown on two layers of stacked graphene covering W coated SiO<sub>2</sub>. (A-1), (A-2) and (A-3) have scale bars of 10, 5, and 0.5 μm, respectively. (B) A diamond film nucleated and grown on three layers of stacked graphene covering W coated SiO<sub>2</sub>. (B-1), (B-2) and (B-3) have scale bars of 10, 5, and 0.5 μm, respectively. (C) A diamond film nucleated and grown on four layers of stacked graphene covering W coated SiO<sub>2</sub>. (C-1), (C-2) and (C-3) have scale bars of 10, 5, and 0.5 μm, respectively. (D) Raman spectra of diamond films shown in (A), (B), and (C). Excitation laser is 532 nm.



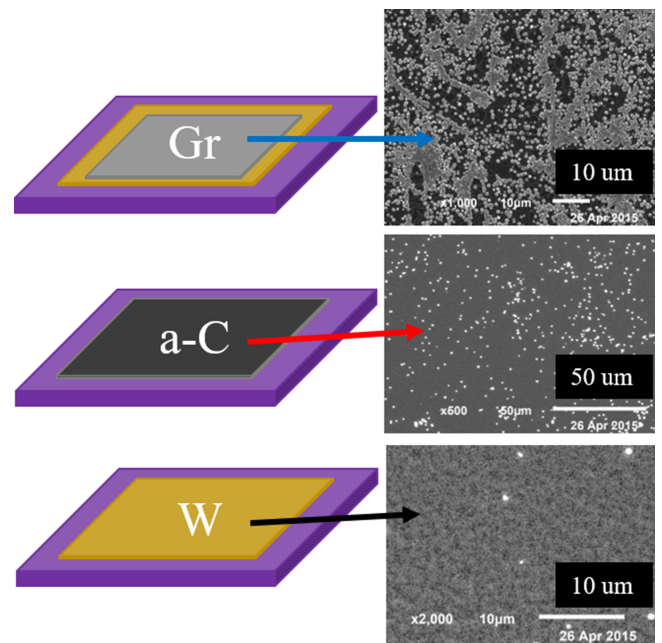
show clear diamond peaks at  $1334\text{ cm}^{-1}$ , which includes a shift by  $2\text{ cm}^{-1}$  from the standard diamond Raman peak at  $1332\text{ cm}^{-1}$ . Stress formed during the merger of individual diamond grains into a continuous diamond film is believed to cause the additional Raman shift. These diamond films are grown by diamond CVD plasma in 3%  $\text{CH}_4$  diluted by 97% hydrogen for 4 hr at a gas pressure of 50 Torr and at a substrate temperature around  $900\text{ }^\circ\text{C}$ .

Based on the distance between diamond nuclei highlighted by a red circle shown in Fig. 2(C), the equivalent diamond nucleation is  $10^{10}\text{ cm}^{-2}$ . Based on the average diamond grain size of less than  $1\text{ }\mu\text{m}$  in the continuous diamond film shown in Fig. 4(C-3), the uniformly distributed diamond nucleation density is higher than  $10^8\text{ cm}^{-2}$ . This paper reports the heterogeneous diamond nucleation based on graphene of only one atom thick. The diamond nucleation density has not been optimized. However, the diamond nucleation without diamond seeding or BEN along monolayer graphene edges is clearly demonstrated.

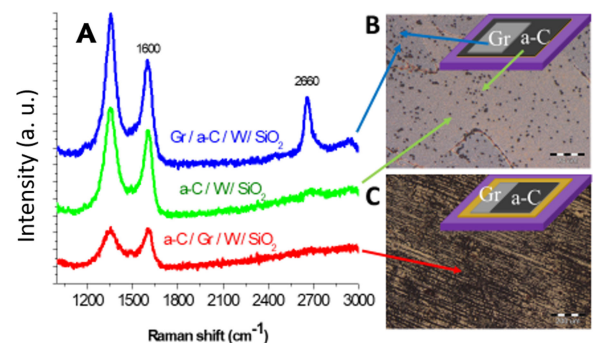
Amorphous carbon has been reported to enhance diamond nucleation on diamond seeded silicon by plasma enhanced chemical vapor deposition [24]. Amorphous carbon was also reported to be convertible to diamond by a laser assisted process [32]. Roles played by carbon in carbon-based diamond nucleation are very much dependent on the detailed process parameters. High-peak-power laser may melt carbon to reach a super undercooling state. Non-diamond carbon is etched by atomic hydrogen from PECVD Plasma to form carbon-containing radicals. These radicals may insert to the carbon clusters again. When the insertion is in the form of  $\text{sp}^3$  carbon-carbon bonds, it will survive the plasma etching environment for a longer period of time compared to non- $\text{sp}^3$  bonded insertion. Atomic hydrogen satisfies dangling bonds formed by breaking undesirable  $\text{sp}^2$  carbon-carbon bonds. Subsequent abstraction of atomic hydrogen frees up active carbon sites for insertion of carbon containing radicals. These processes are in favor of increasing the contents of  $\text{sp}^3$  bonded carbon and, therefore, enhance diamond nucleation.

Figure 5 shows SEM images of diamond nucleation on (i) monolayer graphene covered tungsten, (ii) amorphous carbon, and (iii) tungsten. All three cases use substrates with silicon dioxide surface. The same PECVD parameters apply to all three cases. Fig. 5 clearly shows that unlike monolayer graphene, the coating of an amorphous carbon film on tungsten coated  $\text{SiO}_2$  only results in scarcely distributed diamond nuclei. The diamond nucleation density is much lower than that on monolayer graphene covered and tungsten coated substrate. The unique crystalline structure and edges of monolayer graphene enable the much more effective enhancement of diamond nucleation than amorphous carbon without needing diamond seeding. Tungsten coating alone does not enhance much diamond nucleation by the same PECVD conditions.

Figure 6 shows optical images of diamond nucleation on (i) graphene covered amorphous carbon coating on tungsten coated silicon dioxide, (ii) amorphous carbon coating on



**FIGURE 5.** Schematic diagrams of surface coatings for diamond nucleation and SEM images of diamond particles on the substrates. Diamond nucleation on graphene covered tungsten coated silicon dioxide surface is much more effective than amorphous carbon coated silicon dioxide surface, and tungsten coated silicon dioxide surface.



**FIGURE 6.** (A) Raman spectra of hybrid amorphous carbon coatings stacked in different sequences with graphene tungsten on  $\text{SiO}_2$  and (B, C) Optical micrographs of substrate surface exhibiting little effectiveness in heterogeneous diamond nucleation under the same diamond plasmas CVD conditions used in this work when an additional amorphous carbon film is deposited. Scale bars are  $20\text{ }\mu\text{m}$ .

tungsten coated silicon dioxide, and (iii) amorphous carbon coating on graphene covered tungsten coated silicon dioxide. Amorphous carbon shows little effectiveness in enhancing diamond nucleation in all three cases.

We have compared multi-layer graphene with randomly stacked multiple layers of monolayer graphene. It was confirmed that multi-layer graphene does not enhance diamond nucleation as much as stacked individual monolayer graphene. Based on the experimental observation, we proposed that the underlining tungsten provides favorable conditions for carbon-tungsten  $\text{sp}^3$  bonding to be formed at edges of

graphene in the environments of diamond CVD plasma in methane diluted with hydrogen. Atomic hydrogen termination of dangling bonds helps stabilize the developing diamond nuclei. This sp<sup>3</sup> bonding between carbon and tungsten raises the carbon atom from the tungsten and allow further chain reactions to occur for insertion of additional carbon-containing radicals, leading to chemical nucleation of diamond.

We have demonstrated chemical nucleation of diamond. Edges of monolayer graphene react with underlining tungsten to form C-W sp<sup>3</sup> bonds and convert the 2-D graphene edges into 3-D carbon structure supported by carbon-tungsten bonds. Diamond nucleation can be achieved without applied bias enhancement and direct diamond seeding.

An US patent #10,351,948 was recently awarded for the core idea described in this paper. Transfer-free graphene assisted diamond nucleation (US patent pending) by PECVD on co-sputtered copper films containing tungsten has also been proven feasible. Other metals including molybdenum have also been studied to show diamond nucleation although the tungsten is more effective. These results will be published elsewhere.

#### IV. CONCLUSION

We report chemical nucleation of diamond at edges of monolayer graphene on tungsten. Edges are formed by hydrogen-rich plasma etching of graphene. By randomly stacking layers of monolayer graphene on a tungsten coated substrate, a continuous diamond film is deposited by microwave plasma in hydrogen diluted by hydrogen without resorting to direct diamond seeding and bias enhanced diamond nucleation. For the first time, monolayer graphene enabled diamond nucleation is reported. A chemical diamond nucleation mechanism is proposed based on experimental observations. Hydrogen stabilized sp<sup>3</sup> bonded carbon at graphene edge reacts with tungsten to form sp<sup>3</sup> C-W bonds, which convert 2-D graphene edge into a 3-D sp<sup>3</sup> bonded structure in favor for further chain reactions and insertion of carbon-containing radicals from the plasma. The randomly stacked monolayer graphene results in increased edges of individual layer of monolayer graphene to react with tungsten. The diamond nucleation density increases with the number of layers of randomly stacked monolayer graphene on tungsten. Theoretical confirmation of the proposed diamond nucleation by scientists will help further optimization of this invention as a practical technique in complement with direct diamond seeding and BEN for the deposition of diamond films and related applications.

#### REFERENCES

- [1] K. D. Chabak *et al.*, "Full-wafer characterization of AlGaIn/GaN HEMTs on free-standing CVD diamond substrates," *IEEE Electron Device Lett.*, vol. 31, no. 2, pp. 99–101, Feb. 2010.
- [2] R. Heidinger, G. Dammertz, A. Meier, and M. K. Thumm, "CVD diamond windows studied with low- and high-power millimeter waves," *IEEE Trans. Plasma Sci.*, vol. 30, no. 3, pp. 800–807, Jun. 2002.
- [3] C. M. Flannery, M. D. Whitfield, and R. B. Jackman, "Surface acoustic wave properties of freestanding diamond films," *IEEE Trans. Ultrasonics, Ferroelect., Freq. Control*, vol. 51, no. 3, pp. 368–371, Mar. 2004.
- [4] F. Foulon, T. Pochet, E. Gheeraert, and A. Deneuville, "CVD diamond films for radiation detection," *IEEE Trans. Nucl. Sci.*, vol. 41, no. 4, pp. 927–932, Aug. 1994.
- [5] L. S. Pan *et al.*, "Electrical transport properties of undoped CVD diamond films," *Science*, vol. 255, no. 5046, pp. 830–833, 1992.
- [6] Y. Tzeng, Y.-R. Chen, C.-C. Chang, P.-Y. Li, and Y.-C. Chu, "NV center charge state controlled graphene-on-diamond field effect transistor actions with multi-wavelength optical inputs," *IEEE Open J. Nanotechnol.*, vol. 1, pp. 18–24, 2020, doi: [10.1109/OJNANO.2020.2993007](https://doi.org/10.1109/OJNANO.2020.2993007).
- [7] Y. Tzeng, M. Yoshikawa, F. Murakawa, and M.A., Eds, *Applications of Diamond Films and Related Materials*. Elsevier Science Publishers B.V., Amsterdam, The Netherlands, 1991.
- [8] T.-C. Yang, C.-Y. Chang, A. A. Yarmishyn, Y.-S. Mao, Y.-P. Yang, and M.-L. Wang, "Carboxylated nanodiamond-mediated CRISPR-Cas9 delivery of human retinoschisis mutation into human iPSCs and mouse retina," *Acta Biomaterialia*, pp. 484–494, 2020.
- [9] Y.-W. Cheng *et al.*, "Electrically conductive ultrananocrystalline diamond-coated natural graphite-copper anode for new long life lithium-ion battery," *Adv. Mater.*, pp. 1–6, 2014, doi: [10.1002/adma.201400280](https://doi.org/10.1002/adma.201400280).
- [10] T. S. Huang *et al.*, "Immobilization of antibodies and bacterial binding on nanodiamond and carbon nanotubes for biosensor applications," *Diamond Related Mater.*, vol. 13, no. 4–8, pp. 1098–1102, 2004.
- [11] Y. Mitsuda, Y. Kojima, T. Yoshida, and K. Akashi, "The growth of diamond in microwave plasma under low pressure," *J. Mater. Sci.*, vol. 22, no. 5, pp. 1557–1562, 1987.
- [12] S. Iijima, Y. Aikawa, and K. Baba., "Growth of diamond particles in chemical vapor deposition," *J. Mater. Res.*, vol. 6, no. 7, pp. 1491–1497, 1991.
- [13] M. Ihara, H. Komiyama, and T. Okubo, "Correlation between nucleation site density and residual diamond dust density in diamond film deposition," *Appl. Phys. Lett.*, vol. 65, no. 9, pp. 1192–1194, 1994.
- [14] P. A. Dennig, H. Shiomi, D. A. Stevenson, and N. M. Johnson, "Influence of substrate treatments on diamond thin film nucleation," *Thin Solid Films*, vol. 212, no. 1, pp. 63–67, 1992.
- [15] P. A. Dennig and D. A. Stevenson, "Influence of substrate topography on the nucleation of diamond thin films," *Appl. Phys. Lett.*, vol. 59, no. 13, pp. 1562–1564, 1991.
- [16] J. C. Angus, Y. Wang, and M. Sunkara, "Metastable growth of diamond and diamond-like phases," *Annu. Rev. Mater. Sci.*, vol. 21, no. 1, pp. 221–248, 1991.
- [17] H. Maeda, S. Masuda, K. Kusakabe, and S. Morooka, "Nucleation and growth of diamond in a microwave plasma on substrate pretreated with non-oxide ceramic particles," *J. Cryst. Growth*, vol. 121, no. 3, pp. 507–515, 1992.
- [18] P. Ascarelli and S. Fontana, "Dissimilar Grit-size dependence of the diamond nucleation density on substrate surface pretreatments," *Appl. Surf. Sci.* vol. 64, no. 4, pp. 307–311, 1993.
- [19] Y.-C. C. Chu, Y. Tzeng, and O. Auciello, "Microwave plasma enhanced chemical vapor deposition of nanocrystalline diamond films by bias-enhanced nucleation and bias-enhanced growth," *J. Appl. Phys.*, vol. 115, 2014, Art. no. 024308.
- [20] K. Janischowsky, W. Ebert, and E. Kohn, "Bias enhanced nucleation of diamond on silicon (100) in a HFCVD system," *Diamond Related Mater.*, vol. 12, no. 3, pp. 336–339, 2003.
- [21] Y. Tzeng, S. P. Yeh, W. C. Fang, and Y. C. Chu, "Nitrogen-incorporated ultrananocrystalline diamond and multi-layer-graphene-like hybrid carbon films," *Sci. Rep.*, vol. 4, no. 4531, pp. 1–7, 2014.
- [22] C.-H. Tu, W. Chen, H.-C. Fang, Y. Tzeng, and C. P. Liu, "Heteroepitaxial nucleation and growth of graphene nanowalls on silicon," *Carbon*, vol. 54, pp. 234–240, 2013.
- [23] Y. Tzeng, W. L. Chen, C.-H. Wu, J.-Y. Lo, and C.-Y. Li, "The synthesis of graphene nanowalls on a diamond film on a silicon substrate by direct-current plasma chemical vapor deposition," *Carbon*, vol. 53, pp. 120–129, 2013.
- [24] P. N. Barnes and R. L. C. Wu, "Nucleation enhancement of diamond with amorphous films," *Appl. Phys. Lett.*, vol. 62, no. 1, 1993.
- [25] J. J. Dubray, C. G. Pantano, and W. A. Yarbrough, "Graphite as a substrate for diamond growth," *J. Appl. Phys.*, vol. 72, no. 7, pp. 3136–3141, 1992.
- [26] Z. Li, L. Wang, T. Suzuki, A. Argoitia, P. Pirouz, and J. C. Angus, "Orientation relationship between chemical vapor deposited diamond and graphite substrates," *J. Appl. Phys.*, vol. 73, no. 2, pp. 711–715, 1993.

- [27] W. R. L. Lambrecht, C. H. Lee, B. Segall, J. C. Angus, Z. Li, and M. Sunkarat, "Diamond nucleation by hydrogenation of the edges of graphitic precursors," *Nature*, vol. 364, pp. 607–610, 1993.
- [28] T. Suzuki, M. Yagi, K. Shibuki, and M. Hasemi, "Oriented diamond on graphite flakes," *Appl. Phys. Lett.*, vol. 65, no. 5, Aug. 1994.
- [29] H. Kawarada, C. Wild, N. Herres, R. Locher, P. Koidl, and H. Nagasawa, "Heteroepitaxial growth of highly oriented diamond on cubic silicon carbide," *J. Appl. Phys.*, vol. 81, no. 8, pp. 3490–3493, 1997.
- [30] H. Kawarada, T. Suesada, and H. Nagasawa, "Heteroepitaxial growth of smooth and continuous diamond thin films on silicon substrates via high quality silicon carbide buffer layers," *Appl. Phys. Lett.*, vol. 66, no. 5, pp. 583–585, 1995.
- [31] K. Ohtsuka, K. Suzuki, A. Sawabe, and T. Inuzuka, "Epitaxial growth of diamond on iridium," *Jpn. J. Appl. Phys.*, vol. 35, pp. L1072–L1074, 1996.
- [32] J. Narayana and A. Bhaumik, "Research update: Direct conversion of amorphous carbon into diamond at ambient pressures and temperatures in air," *APL Mater.*, vol. 3, 2015, Art. no. 100702.
- [33] A. Haque, R. Sachan, and J. Narayan, "Synthesis of diamond nanostructures from carbon nanotube and formation of diamond-CNT hybrid structures," *Carbon*, vol. 150, pp. 388–395, 2019.
- [34] S. Skokov, B. Weiner, and M. Frenklach, "Elementary reaction mechanism for growth of diamond (100) surfaces from methyl radicals," *J. Phys. Chem.*, vol. 98, pp. 7073–7082, 1994.
- [35] P. C. Redfern, D. A. Horner, L. A. Curtiss, and D. M. Gruen, "Theoretical studies of growth of diamond (110) from dicarbon," *J. Phys. Chem.*, vol. 100, pp. 11654–11663, 1996.
- [36] D. M. Gruen, P. C. Redfern, D. A. Horner, P. Zapol, and L. A. Curtiss, "Theoretical studies on nanocrystalline diamond: Nucleation by dicarbon and electronic structure of planar defects," *J. Phys. Chem. B*, vol. 103, pp. 5459–5467, 1999.
- [37] L. T. Sun, J. L. Gong, Z. Y. Zhu, D. Z. Zhu, S. X. He, and Z. X. Wang, "Nanocrystalline diamond from carbon nanotube," *Appl. Phys. Lett.*, vol. 84, no. 15, pp. 2901–2903, 2004.
- [38] X. S. Sun *et al.*, "The effect of ion bombardment on the nucleation of CVD diamond," *Diamond Related Mater.*, vol. 8, pp. 1414–1417, 1999.
- [39] A. Haque, P. Pant, and J. Narayan, "Large-area diamond thin film on Q-carbon coated crystalline sapphire by HFCVD," *J. Cryst. Growth*, vol. 504, pp. 17–25, 2018.
- [40] S. Yugo, T. Kanai, T. Kimura, and T. Muto, "Generation of diamond nuclei by electric field in plasma chemical vapor deposition," *Appl. Phys. Lett.*, vol. 58, no. 10, pp. 1036–1038, 1991.
- [41] S. D. Wolter *et al.*, "Textured growth of diamond on silicon via in situ carburization and Was-enhanced nucleation," *Appl. Phys. Lett.*, vol. 62, no. 11, pp. 1215–1217, 1993.
- [42] A. Joseph, C. Tanger, J. Wei, and Y. Tzeng, "Diamond coated quartz and sapphire optical windows," *Diamond Films Technol.*, vol. 5, no. 2, pp. 87–93, 1995.
- [43] M. Kawarada, K. Kurihara, and K. Sasaki, "Diamond synthesis on a metal substrate," *Diamond Related Mater.*, vol. 2, pp. 1083–1089, 1993.
- [44] A. Veillere *et al.*, "Influence of WC-Co substrate pretreatment on diamond film deposition by laser-assisted combustion synthesis," *ACS Appl. Mater. Interfaces*, vol. 3, pp. 1134–1139, 2011.
- [45] Y. Hirose and K. Komaki, "Vapor-phase method for synthesis of diamond," US patent, vol. 4, no. 938, 1990. 92, Art. no. 940.
- [46] R. Phillips, J. Wei, and Y. Tzeng, "High quality flame-deposited diamond films for IR optical windows," *Thin Solid Films.*, vol. 212, no. 1–2, pp. 30–34, 1992.
- [47] D. R. McKenzie, "Tetrahedral bonding in amorphous carbon," *Rep. Prog. Phys.*, vol. 59, pp. 1611–1664, 1996.
- [48] K. Suzuki, A. Sawabe, H. Yasuda, and T. Inuzuka, "Growth of diamond thin films by dc plasma chemical vapor deposition," *Appl. Phys. Lett.*, vol. 50, no. 12, 1987, Art. no. 728.
- [49] B. Wei *et al.*, "The transformation of fullerenes into diamond under different processing conditions," *J. Mater Proc Tech.*, vol. 63, pp. 573–557, 1997.
- [50] J. Narayan, A. Bhaumik, R. Sachan, A. Haque, S. Gupta, and P. Panta, "Direct conversion of carbon nanofibers and nanotubes into diamond nanofibers and the subsequent growth of large-sized diamonds," *Nanoscale*, vol. 11, 2019, Art. no. 2238.
- [51] P. V. Bakharev *et al.*, "Chemically induced transformation of chemical vapour deposition grown bilayer graphene into fluorinated single-layer diamond," *Nat. Nanotechnol.*, vol. 15, pp. 59–66, 2020.
- [52] M. Peplow, "Artificial retina gets diamond coating," *Nat. Online*, vol. 31, Mar. 2005, doi:10.1038/news050328-9.
- [53] P. V. Bakharev *et al.*, "Chemically induced transformation of chemical vapour deposition grown bilayer graphene into fluorinated single-layer diamond," *Nat. Nanotechnol.*, 2019, doi:10.1038/s41565-019-0582-z.
- [54] F. Piazza *et al.*, "Low temperature, pressureless sp<sup>2</sup> to sp<sup>3</sup> transformation of ultrathin, crystalline carbon films," *Carbon*, vol. 145, pp. 10–22, 2019.
- [55] D. De Fazio *et al.*, "High-mobility, wet-transferred graphene grown by chemical vapor deposition," *ACS Nano*, vol. 13, no. 8, pp. 8926–8935, 2019.
- [56] Y. Tzeng, C - C. Chang P - Y. Li, and Y - C. Chu, "Graphene optoelectronic detector and method for detecting photonic and electromagnetic energy by using the same," US patent #9, 620597 B2, Apr. 11, 2017.
- [57] Y. Tzeng and W - L. Chen, "Method of transferring a graphene film," US Patent #9,181,100, Nov. 10, 2015.



**YONHUA TZENG** (Fellow, IEEE) received the B.S. degree in electrical engineering from National Taiwan University, Taipei, Taiwan in 1977 and M.S. and Ph.D. degrees in electrical and computer engineering from Texas Tech University, Lubbock, TX, USA in 1981 and 1983, respectively.

He is a University Chair and Distinguished Professor, with the Institute of Microelectronics, Department of Electrical Engineering, National Cheng Kung University, Tainan, Taiwan. He is a Former Vice President for Research and Development, Dean of College of Electrical Engineering and Computer Science, and Director of Center of Micro-Nano Science and Technology with National Cheng Kung University. Before joining NCKU, he was an Alumni Chair Professor and Associate Director with Alabama Micro-Nano Science and Technology Center, Auburn University, Auburn, Alabama USA. He has authored or coauthored more than 200 referred papers and been awarded 45 patents.

Professor Tzeng is an Inaugural Senior Member of US National Academy of Inventors, a Fellow of IEEE associated with Electron Device Society, Industrial Electronics Society and Nanotechnology Council. He was the President from 2018 to 2019 and is immediate Past President from 2020 to 2021 of IEEE NANOTECHNOLOGY COUNCIL.



**CHIH-CHUN CHANG** received the M.S. degree in electrical engineering from National Cheng Kung University, Tainan, Taiwan in 2015. He has since been working as an Engineer with the semiconductor industry.